Chapter 12
Climate Change Impact on Agricultural Water Resources Variability in the Northern Highlands of Ethiopia

Shimelis G. Setegn, David Rayner, Assefa M. Melesse, Bijan Dargahi, Ragahavan Srinivasan, and Anders Wörman

Abstract The economy of Ethiopia mainly depends on agriculture, and this in turn largely depends on available water resources. A major effect of climate change is likely to be alterations in hydrologic cycles and changes in water availability. This chapter reports the use of global climate models (GCM's) and application of a hydrological model to investigate agricultural water resources' sensitivity to climate change in the Lake Tana Basin, Ethiopia. Projected changes in precipitation and temperature in the basin for two future seasons (2046–2065 and 2080–2100) were analyzed using outputs from fifteen GCMs. A historical-modification procedure was used to downscale large scale outputs from four GCM models to watershed-scale climate data. The study then investigated how these changes in temperature and precipitation might translate into changes in streamflow and other hydrological components using SWAT model. We interpret the different aspects of the hydrological responses to imply that changes in runoff and other hydrological variables could be significant, even though the GCMs do not agree on the direction of the change indicating high uncertainty.

Keywords Climate change impact · Lake Tana · SWAT · Hydrological modeling · GCM · Downscaling · SRES

12.1 Introduction

Climate changes pose significant economic and environmental risks worldwide. The economy of Ethiopia mainly depends on agriculture, and this in turn largely depends on available water resources. The country has a fragile highland ecosystem that is currently under stress due to increasing population pressure and land degradation. The Blue Nile River basin is one of the most sensitive basins to changing climate and water resources variability in the region (Kim and Kaluarachchi, 2009). But as

S.G. Setegn (✉)
Department of Earth and Environment, Florida International University, Miami, FL 33199, USA
e-mail: ssetegn@fiu.edu

A.M. Melesse (ed.), *Nile River Basin*, DOI 10.1007/978-94-007-0689-7_12,

yet, there is no consensus on the effect of climate change on water availability in the region. Hence it is necessary to improve our understanding of the problems caused by the changing climate.

In recent years, concern has increased over climate change caused by increasing concentrations of carbon dioxide and other trace gases in the atmosphere. A major effect of climate change is likely to be alterations in hydrologic cycles and changes in water availability. Increased evaporation, combined with changes in precipitation, has the potential to affect runoff, the frequency and intensity of floods and droughts, soil moisture, and available water for irrigation and hydroelectric generation. In addition, watershed hydrology is affected by vegetation types, soil properties, geology, terrain, land use practices, and the spatial pattern of interactions among these factors and with climate (Richey et al., 1989; Laurance, 1998; Schulze, 2000; Fohrer et al., 2001; Zhang et al., 2001; Huang and Zhang, 2004, Brown et al., 2005, van Roosmalen et al., 2009, Tu, 2009). The Intergovernmental Panel on Climate Change's (IPCC, 2007) findings suggests that developing countries like Ethiopia will be more vulnerable to climate change due to their economic, climatic and geographic settings. According to IPPC (2007) report, the population at risk of increased water stress in Africa is projected to be between 75–250 and 350–600 million people by the 2020s and 2050s, respectively. Moreover, yields from rain-fed agriculture could be reduced by up to 50%, in countries which depend mainly on rain-fed agriculture.

Assessing the impact of climate change on stream flows, soil moisture, groundwater and other hydrological parameters essentially involves taking projections of climatic variables (e.g., precipitation, temperature, humidity, mean sea level pressure etc.) at a global scale, downscaling these global-scale climatic variables to local-scale hydrologic variables, and computing hydrological components for water resources variability and risks of hydrologic extremes in the future. Projections of climatic variables globally have been performed with General Circulations Models (GCMs), which provide projections at large spatial scales. Such large-scale climate projections must then be downscaled to obtain smaller-scale hydrologic projections using appropriate linkages between the local climates. A number of studies have investigated downscaling methods for establishing a connection between coarse-resolution GCMs and hydrologic models (e.g. Wilby et al., 1998, 2000; Hay and Clark, 2003; Wood et al., 2004; Benestad et al. 2008).

There are limited climate change impact studies in Ethiopia (Tarekegn and Tadege, 2006; Kim and Kaluarachchi, 2008; Abdo et al., 2009; Melesse et al., 2009, Beyene et al., 2010). To make a conclusion about the effect of climate change on the watershed hydrology using a particular GCM may not give clear representation of the future changes. According to IPCC (2007), high uncertainty is expected in climate change impact studies if the simulation results of a single GCM are relied upon (IPCC, 1999). To minimize uncertainties due to GCM model formulations and assumptions, this study downscaled outputs from 15 GCMs. This enabled us to show the future hydrological response to a range of possible changes, as expressed by the outputs from the different models. This study chose to generate daily climate projections by modifying the historical datasets to represent the changes in the GCM climatologies.

From among the different Special Report on Emissions Scenarios (SRES), which were developed by the IPCC, this study used the AlB, A2 and B2 scenarios for this climate change impact study. These scenarios cover a range of future pathways, with respect to global vs. regional development, and environmental vs. economic emphases.

Different studies have been conducted to assess the impact of climate change on hydrology in different parts of the world (Gleick and Chalecki, 1999; Neff et al., 2000; Groisman et al., 2001; Chang et al., 2003; Novotny and Stefan, 2007, Kim and Kaluarachchi, 2009; Abdo et al., 2009). Many of these studies indicated water resource variability associated with climate change.

In this study, we investigated the possible effects of climate change on water resources in Lake Tana Basin, Ethiopia by analyzing outputs from GCM models. To get an indication of the consistency of the projected changes in the region, we first compared projected changes in precipitation and temperature across 15 models for two seasons. The study then investigated how changes in temperature and precipitation might translate into changes in stream flow and other hydrological components, using outputs from the four selected climate models. The physically based Soil Water Assessment Tool (SWAT) model was used to determine the impact of climate change on the surface and ground water resources availability in the Lake Tana Basin. The SWAT model was calibrated and validated using historical data from four rivers which flow into Lake Tana: Gumera, Gilgel Abay, Megech and Ribb rivers (Setegn et al., 2009a).

12.2 Materials and Methods

12.2.1 Study Area

Lake Tana is located in the country's north-west highlands (Lat 12°0′ North, Lon 37°15′ East) (Fig. 12.1). The Lake Tana basin comprises an area of 15,096 km^2, including the lake area. The mean annual rainfall of the catchment area is about 1,280 mm. The climate of the region is "tropical highland monsoon" with the main rainy season between June and September. The air temperature shows large diurnal but small seasonal changes with an annual average of 20°C. The mean annual relative humidity (1961–2004) at Bahr Dar meteorological station is 0.65. Lake Tana occupies a wide depression in the Ethiopian plateau. The lake is shallow, oligotrophic, and freshwater, with weak seasonal stratification (Wood and Talling, 1988; Wudneh, 1998). The lake is believed to have been formed due to damming by lava flow during the Pliocene (Mohr, 1962), but the formation of the depression itself started in the Miocene (Chorowiz et al., 1998). Lake Tana basin comprises a total area of 15,096 km^2 (drainage plus lake area). It is rich in biodiversity with many endemic plant species and cattle breeds; it contains large areas of wetlands; it is home to many endemic birds and cultural and archaeological sites. This basin is of critical national significance as it has great potential for irrigation, hydroelectric power, high value crops and livestock production, ecotourism and more.

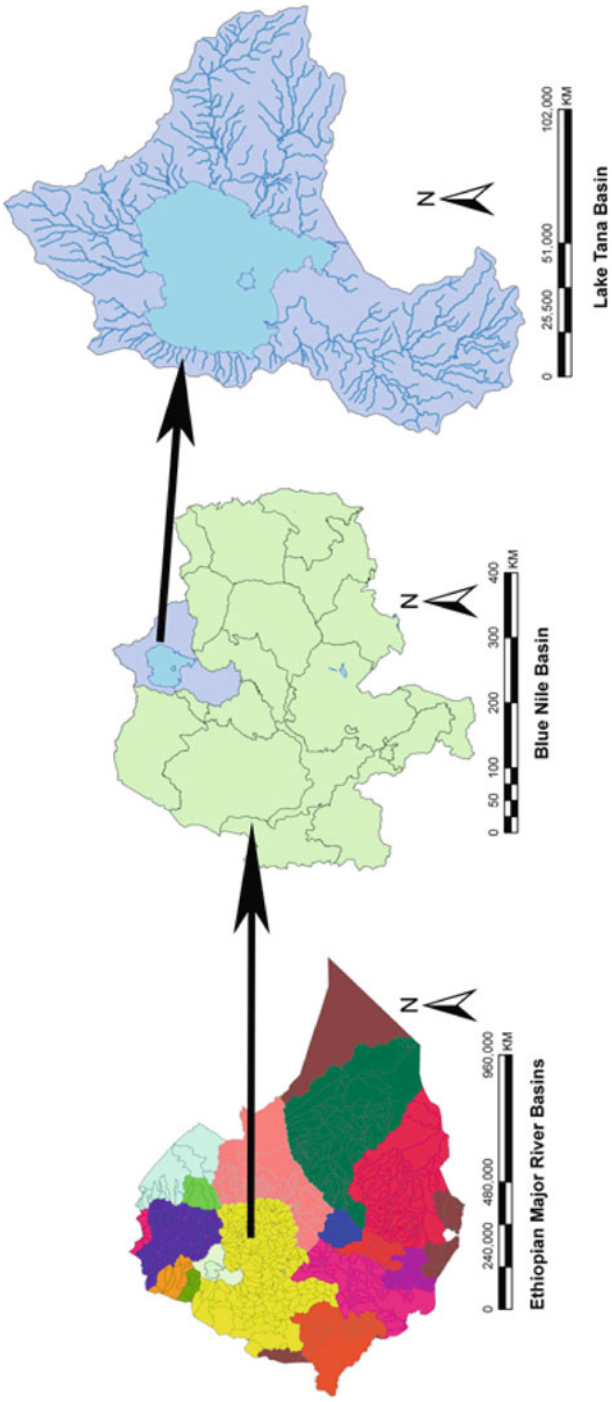

Fig. 12.1 Location Map of the study area

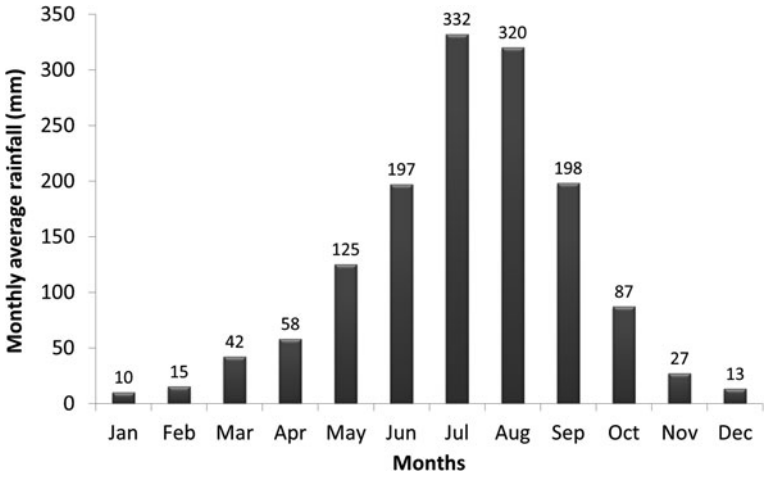

Fig. 12.2 Upper Blue Nile basin monthly average Rainfall (1960–2002)

The lake is a natural type which covers 3,000–3,600 km^2 area at an elevation of 1,800 m and with a maximum depth of 15 m. It is approximately 84 km long, 66 km wide. It is the largest lake in Ethiopia and the third largest in the Nile Basin. Gilgel Abay, Ribb, Gumera and Megech are the main rivers feeding the lake, and contribute more than 90% of the inflow. The Lake is the main source of the Blue Nile River, which is the only surface outflow for the Lake. The climate of the study area varies from humid to semiarid. Most precipitation occurs in the wet season (locally called *Kiremt*) from June to September. The two other seasons are known as *Bega* (normally dry; from October to February) and *Belg* (normally mild; from March to May). About 70% of annual precipitation is concentrated on Kiremt. The annual precipitation has an increasing trend from northeast to southwest. Figure 12.2 shows basin-wide monthly rainfall average. The estimated mean annual precipitation of the study area ranges from 1,200 to 1,600 mm based on data from 1961 to 2000 depending on the studies (Gamachu, 1977; Conway, 1997; Conway, 2000; UNESCO, 2004; Kim et al., 2008, Setegn et al., 2009a). Due to the summer monsoon occurring between June and September, more than 80% of the annual flow occurs from July to October and flows to the downstream countries due to the absence of storage capacity. The observational record from 1980 to 2000 shows a seasonal variation of less than 2°C. The annual mean actual evapotranspiration and water yield of the catchment area are estimated to be 773 and 392 mm, respectively (Setegn et al., 2009a).

12.2.2 General Circulation Models (GCMs)

GCM's are numerical coupled models that represent various earth systems including the atmosphere, oceans, land surface and sea-ice and offer considerable potential for the study of climate change and variability. They numerically simulate changes in climate as a result of slow changes in some boundary conditions (such as the

solar constant) or physical parameters (such as the greenhouse gas concentration) (Abbaspour et al., 2009).

GCM output data were obtained from the World Climate Research Programme's (WCRP's) Coupled Model Inter-comparison Project phase 3 (CMIP3) multi-model dataset. The details of the models used in this study are listed in Table 12.1. Monthly precipitation and average surface air temperatures were used to quantify the range of the projected climate changes for the region. A single run was downloaded for each scenario, and data extracted for the pixel containing the observation stations.

Daily data were extracted from the outputs of four models (cccma_cgcm3_1, gfdl_cm2_1, mpi_echam5, and ncar_ccsm3_0). These data were used for the hydrological modeling and assessing the impact of climate change on stream flows, soil moisture, ground water and other hydrological parameters in the Lake Tana basin.

Table 12.1 The details of the different GCM are used in this study and their spatial resolutions (IPCC, 2007)

Center	Model	Atmospheric resolution (approx)
Bjerknes Centre for Climate Research Norway (BCCR)	Bergen Climate Model (BCM2.0)	2.8° × 2.8°
Canadian Center for Climate Modelling and Analysis Canada (CCCMA)	Coupled Global Climate Model (CGCM3)	3.75° × 3.7°
Centre National de Recherches Meteorologiques France (CNRM)	CNRM-CM3	2.8° × 2.8°
Australia's Commonwealth Scientific and Industrial Research Organisation Australia (CSIRO)	CSIRO Mark 3.0	1.9° × 1.9°
Australia's Commonwealth Scientific and Industrial Research Organisation Australia (CSIRO)	CSIRO Mark 3.5	1.9° × 1.9°
Max-Planck-Institut for Meteorology Germany (MPI-M)	ECHAM5/MPI-OM	1.9° × 1.9°
Meteorological Institute of the University of Bonn (Germany) (MIUB)	ECHO-G	3.75° × 3.7°
Geophysical Fluid Dynamics Laboratory USA (GFDL)	CM2.0 – AOGCM	2.5° × 2.0°
Geophysical Fluid Dynamics Laboratory USA (GFDL)	CM2.1 – AOGCM	2.5° × 2.0°
Institute for Numerical Mathematics Russia (INM)	INMCM3.0	5.0° × 4.0°
Institut Pierre Simon Laplace France (IPSL)	IPSL-CM4	3.75° × 2.5°
Meteorological Research Institute Japan (MRI)	MRI-CGCM2.3.2	2.8° × 2.8°
National Centre for Atmospheric Research USA (NCAR)	Parallel Climate Model (PCM)	2.8° × 2.8°
National Centre for Atmospheric Research USA (NCAR)	Community Climate System Model, version 3.0 (CCSM3)	1.4° × 1.4°
Hadley Centre for Climate Prediction and Research, Met Office, United Kingdom – UK Met. Office UK (UKMO)	HadCM3	3.75° × 2.5°

Monthly outputs of fifteen GCMs were used for the analysis of changes in major climate variables (precipitation, minimum and maximum temperature) in the Lake Tana basin. The models are the Bergen Climate Model (BCM2.0), Coupled Global Climate Model (CGCM3), CNRM-CM3, CSIRO Mark 3.0, ECHAM5/MPI-OM, ECHO-G, CM2.0 – AOGCM, CM2.1 – AOGCM, INMCM3.0, IPSL-CM4, MRI-CGCM2.3.2, Parallel Climate Model (PCM), Community Climate System Model, version 3.0 (CCSM3) and HadCM3 Global climate change models.

12.2.3 Climate Change Scenarios

Scenarios are images of the future, or alternative futures. They are neither predictions nor forecasts. Rather, each scenario is one alternative image of how the future might unfold. A set of scenarios assists in the assessment of future developments in complex systems that are either inherently unpredictable, or that have high scientific uncertainties (IPCC, 2007).

The Special Report on Emissions Scenarios (SRES) (IPCC, 2007) are grouped into four scenario families (A1, A2, B1 and B2) that explore alternative development pathways, covering a wide range of demographic, economic and technological driving forces and resulting GHG emissions. The A1 storyline assumes a world of very rapid economic growth, a global population that peaks in mid-century and rapid introduction of new and more efficient technologies. Scenario A1 is divided into three groups that describe alternative directions of technological change: fossil intensive (A1FI), non-fossil energy resources (A1T) and a balance across all sources (A1B). The SRES A1B Emissions Scenarios (a scenario in A1 family) describes "a future world of very rapid economic growth, global population that peaks in mid-century and declines thereafter, and rapid introduction of new and more efficient technologies". Scenario B1 describes a convergent world, with the same global population as A1, but with more rapid changes in economic structures toward a service and information economy with reductions in materials intensity, and the introduction of clean and resource efficient technologies. B2 describes a world with intermediate population and economic growth, emphasizing local solutions to economic, social, and environmental sustainability. Scenario A2 describes a very heterogeneous world with high population growth, slow economic development and slow technological change. No likelihood has been attached to any of the SRES scenarios (IPCC, 2007). In this study three SRES scenarios (A1B, B1, and A2) were used. These scenarios were constructed to explore future developments in the global environment with special reference to the production of greenhouse and aerosol precursor emissions. Each scenario assumes a distinctly different direction for future developments.

12.2.4 Downscaling Methods

GCM's are coarse in resolution and are unable to resolve significant sub-grid scale features such as topography, clouds and land use (Grotch and MacCracken, 1991).

For instance, the Canadian Center for Climate Modeling and Analysis Canada (CCCMA), Coupled Global Climate Model (CGCM3) is resolved at a spatial resolution of 3.75° longitude by 3.7° latitude; the Hadley Centre for Climate Prediction and Research HadCM3 model is resolved at a spatial resolution of 3.75° longitude by 2.5° latitude, and so on. Table 12.1 above shows the different models and their spatial resolutions. There is a significant gap between the large spatial resolution GCMs and regional and local watershed processes. This scale mismatch causes a considerable problem for the assessment of climate change impact using hydrological models. Hence, significant attention should be given to the development of downscaling methodologies for obtaining high-resolution climate or climate change information from relatively coarse-resolution global climate models (GCMs). This will help for better prediction of climate change consequences at hydrological scale.

Basically, there are two main approaches available for the downscaling of large spatial resolution GCM outputs to a finer spatial resolution, termed dynamical and statistical downscaling. In dynamical downscaling, a higher resolution climate model or regional climate model is forced using a GCM. The statistical approach establishes empirical relationships between GCM-resolution climate variables and local climate.

Statistical downscaling is a tool for downscaling climate information from coarse spatial scales to finer scales. The underlying concept is that local climate is conditioned by large-scale climate and by local physiographical features such as topography, distance to a coast, and vegetation. At a specific location, therefore, links should exist between large-scale and local climatic conditions. Statistical downscaling consists of identifying empirical links between large-scale patterns of climate elements (predictors) and local climate (the predictand), and applying them to output from global or regional models. Successful statistical downscaling is thus dependent on long, reliable series of predictors and predictands. Different studies have shown that the two downscaling methods are usually similar for present day climate, while differences in future climate projections are found more frequently. These differences can be explained by the unwise choice of predictors in the statistical downscaling, for example, predictors that carry the climate signal. It has also been suggested that results from statistical downscaling may be misleading because the projected climate change exceeds the range of data used to develop the model. However, differences between results from statistical downscaling and regional modeling may also result from the ability of statistical downscaling to reproduce local features that are not resolved in the regional models (Draggan, 2010). Major disadvantages of statistical downscaling versus using regional climate model includes: the assumption that observed links between large-scale predictors and local predictands will persist in a changed climate, and difficulties in reproducing observed autocorrelations within climate time-series at daily time-scales. Statistical downscaling does not necessarily produce a physically sound relationship between different climate elements. Similarly some advantages of statistical downscaling versus regional modeling includes: statistical downscaling is less technically

demanding than regional modeling; it is thus possible to downscale from several GCMs and several different emissions scenarios relatively quickly and inexpensive; it is possible to tailor scenarios for specific localities, scales, and problems. The spatial resolution applied in regional climate modeling is still too coarse for many impact studies, and some variables are either not available or not realistically reproduced by regional models.

This study generated daily climate projections by modifying the historical datasets to represent changes in the GCM climatologies. This is different from the approach more usually thought of as "statistical downscaling" (e.g. Benestad et al., 2008) where scenarios are created as a function of the daily outputs from GCMs themselves. The historical-modification approach was used because hydrological models often perform poorly when applied to datasets with distributions of daily climate data that are different from their training data, and statistical downscaling techniques often result in distributions that are noticeably different from observed time-series (e.g. with compressed variance).

This study followed the historical-modification procedure of Harrold and Jones (2003) which produces climate time-series and that have similar statistical properties to the observed datasets. In summary, this method involved calculating the difference between the daily cumulative-frequency-distributions (CFDs) of a GCM output variable for a present-day period and a future period, and then applying these differences to an observed dataset. This simple "downscaling" technique is a good compromise between the requirement to produce realistic time-series, and the desire to represent the effects of climate change across different weather situations, as these are simulated in the GCMs. In addition, the method is easy to implement and fast to run. It is a good solution for producing climate change scenarios for impact assessments.

Our implementation of the Harrold and Jones method was as follows. Cumulative-frequency-distributions for daily precipitation, maximum and minimum temperatures were first calculated for the GCM outputs. The CFDs were calculated independently for each month-of-year, using data from that month-of-year and the preceding and subsequent months. The differences between the present-day period CFD and the scenario-period CFDs were then determined for the cumulative frequencies 0.05, 0.15, 0.25. . .1.0. Absolute differences were calculated for minimum and maximum temperature CFDs, while for precipitation the changes were derived as ratios with-respect-to the present-period values. Because fractional changes in the low-rainfall end of the CFDs may be large, all GCM rainfall values <0.1 mm/day were considered to be zero, and zero values were omitted from the CDF calculations. The extremes of the CFDs (e.g. 0.001, 0.999) were deliberately not sampled. The time windows used are not long enough to define the tails of the CFDs, or changes in them. The changes in the CFDs sampled at cumulative frequencies 0.05–0.95 were then linearly interpolated and extrapolated to cover the entire cumulative frequency range (0–1). Finally, the historical data were ranked and modified to reflect the changes in the GCM CFDs for each scenario and time-period. The result is "downscaled", daily climate time-series.

12.2.5 SWAT Model Description

SWAT (Soil Water Assessment Tool) is continuous time, spatially distributed model designed to simulate water, sediment, nutrient and pesticide transport at a catchments scale on a daily time step. It is one of the watershed models that play a major role in analyzing the impact of land management practices on water, sediment, and agricultural chemical yields in large complex watersheds. It is a public domain model developed by Arnold et al. (1998). SWAT uses hydrologic response units (HRUs) to describe spatial heterogeneity in terms of land cover, soil type and slope within a watershed. The SWAT system is embedded within a geographic information system (GIS) that can integrate various spatial environmental data including soil, land cover, climate and topographic features. Currently, SWAT is embedded in an ArcGIS interface called ArcSWAT. The Simulation of the hydrology of a watershed is done in two separate divisions. One case is the land phase of the hydrological cycle that controls the amount of water, sediment, nutrient and pesticide loadings to the main channel in each subbasin. The second division is routing phase of the hydrologic cycle that can be defined as the movement of water, sediments, nutrients and organic chemicals through the channel network of the watershed to the outlet. In the land phase of hydrological cycle, SWAT simulates the hydrological cycle based on the water balance equation.

$$SW_t = SW_0 + \sum_{i=1}^{t} \left(R_{day} - Q_{surf} - E_a - w_{seep} - Q_{gw}\right) \tag{12.1}$$

In which SW_t is the final soil water content (mm), SW_o is the initial soil water content on day i (mm), t is the time (days), R_{day} is the amount of precipitation on day i (mm), Q_{surf} is the amount of surface runoff on day i (mm), E_a is the amount of evapotranspiration on day i (mm), W_{seep} is the amount of water entering the vadose zone from the soil profile on day i (mm), and Q_{gw} is the amount of return flow on day i (mm).

To estimate surface runoff two methods are available. These are the SCS curve number procedure USDA Soil Conservation Service (USDA, 1972) and the Green & Ampt infiltration method (Green and Ampt, 1911) In this study, the SCS curve number method was used to estimate surface runoff. Hargreaves method was used for estimation of potential evapotranspiration (PET) (Hargreaves, 1985). The SCS curve number is described by equation 12.2.

$$Q_{surf} = \frac{(R_{day} - 0.2S)^2}{(R_{day} + 0.8S)} \tag{12.2}$$

In which, Qsurf is the accumulated runoff or rainfall excess (mm), R_{day} is the rainfall depth for the day (mm), S is the retention parameter (mm). The retention parameter is defined by equation 12.3.

$$S = 25.4\left(\frac{100}{CN} - 10\right) \tag{12.3}$$

The SCS curve number is a function of the soil's permeability, land use and antecedent soil water conditions. SCS defines three antecedent moisture conditions: 1 – dry (wilting point), 2 – average moisture, and 3 – wet (field capacity). The moisture condition 1 curve number is the lowest value that the daily curve number can assume in dry conditions. The curve numbers for moisture conditions 2 and 3 are calculated from equations 12.4 and 12.5.

$$CN_1 = CN_2 - \frac{20 \cdot (100 - CN_2)}{(100 - CN_2 + \exp\left[2.533 - 0.0636 \cdot (100 - CN_2)\right])} \tag{12.4}$$

$$CN_3 = CN_2 \cdot \exp\left[0.00673 \cdot (100 - CN_2)\right] \tag{12.5}$$

In which CN_1 is the moisture condition 1 curve number, CN_2 is the moisture condition 2 curve numbers, and CN_3 is the moisture condition 3 curve numbers.

Typical curve numbers for moisture condition 2 are listed in various tables (Neitsch et al., 2005) which are appropriate to slope less than 5%. But in the Lake Tana basin there are areas with slopes greater than 5%. To adjust the curve number for higher slopes an equation developed by (Williams, 1995) was used (equation 12.6)

$$CN_{2S} = \frac{(CN_3 - CN_2)}{3} \cdot \left[1 - 2 \cdot \exp(-13.86 \cdot slp)\right] + CN_2 \tag{12.6}$$

In which CN_{2S} is the moisture condition 2 curve number adjusted for slope, CN_3 is the moisture condition 3 curve number for the default 5% slope, CN_2 is the moisture condition 2 curve number for the default 5% slope, and slp is the average percent slope of the sub-basin.

The different components of the SWAT model application to the Lake Tana basin are described by Setegn et al. (2009a, 2009b, 2010). More detailed descriptions of the different model components are listed in Neitsch et al. (2005). A comprehensive review of SWAT model applications is given by Gassman et al. (2007).

12.2.6 Hydrological Model Input and Setup

The spatially distributed data needed for the ArcSWAT interface include the Digital Elevation Model (DEM), soil data, land use and stream network layers. Data on weather and river discharge were also used for prediction of streamflow and calibration purposes. For the setup of the SWAT model, we have used a 90 m resolution DEM for the delineation of the watershed and to analyze the drainage patterns of the land surface terrain. Sub-basin parameters such as slope gradient, slope length of the terrain, and the stream network characteristics such as channel slope, length,

and width were derived from the DEM. The soil and land use data were used for the definition of the hydrological response units (HRUs). SWAT model requires different soil textural and physico-chemical properties such as soil texture, available water content, hydraulic conductivity, bulk density and organic carbon content for different layers of each soil type. These data were obtained mainly from the following sources: Soil and Terrain Database for northeastern Africa CD-ROM (Food and Agriculture Organization of the United Nations (FAO), 1998), Major Soils of the world CD-ROM (FAO, 2002), Digital Soil Map of the World and Derived Soil Properties CD-ROM (FAO, 1995), Properties and Management of Soils of the Tropics CD-ROM (Van Wambeke, 2003), Abbay River basin Integrated Development Master Plan Project – Semi detailed Soil Survey and the Soils of Anjeni Area, Ethiopia (SCRP report). Figure 12.3 (left) shows the major soil types in the basin.

The land use map of the study area was obtained from the Ministry of Water Resources, Ethiopia. We have reclassified the land use map of the area based on the available topographic map (1:50,000), aerial photographs and satellite images. The reclassification of the land use map was done to represent the land use according to specific land cover types such as type of crop, pasture and forest. Figure 12.3 (right) shows that more than 50% of the Lake Tana watershed is used for agriculture.

SWAT requires daily meteorological data that can either be read from a measured data set or be generated by a weather generator model. The weather variables used in this study for driving the hydrological balance are daily precipitation, minimum and maximum air temperature for the period 1978–2004. These data were obtained from Ethiopian National Meteorological Agency (NMA) for stations located within and around the watershed.

The daily river discharge data were used for model calibration and validation. The river discharges were characterized with high flow periods during June-September and low flow periods during the rest of the year. The highest discharges were for the Gilgel Abay and Gumera Rivers. Daily river discharge values for the Ribb, Gumera, Gilgel Abay, and Megech Rivers and the outflow Blue Nile (Abbay) River were obtained from the Hydrology Department of the Ministry of Water Resources of Ethiopia. The daily river discharges at four tributaries of Lake Tana (Gumera, Gilgel Abay, Megech and Ribb Rivers) from gauging stations were used for model calibration and validation. The peak flows for all inflow rivers occur in August. But the outflow river gets its peak flow at the month of September. There is a 1 month delay of peak flow for outflow from the Blue Nile River. This is due to the influence of the lake, which retards the flow before it reaches the outlet. The record of the outflow river (Abbay) at Bahir Dar gauge station was not used for model calibration and validation. This is because we have seen a significant difference between the default simulated and measured stream flow data at this gauge station. There is abstraction of water from the lake for irrigation and other purposes. But there is no available information on the amount of water losses from the lake.

The details of the input data used for the setup of the SWAT model are documented in Setegn et al. (2009a).

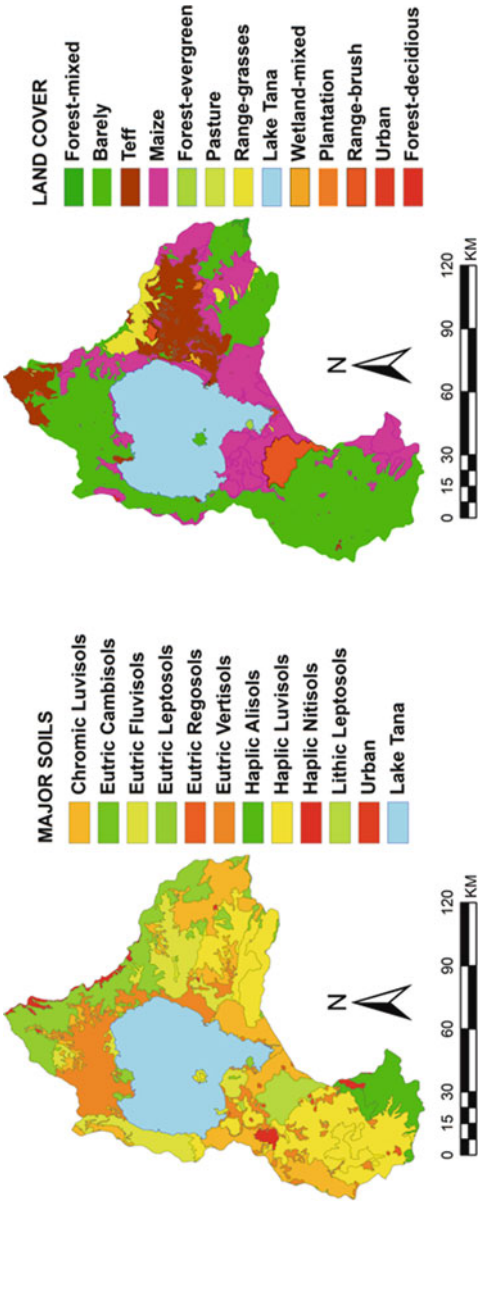

Fig. 12.3 Soil and land use/land cover map of Lake Tana basin

12.2.7 Model Setup, Calibration and Evaluation of SWAT Model

The model setup involved five steps: (1) data preparation, (2) sub-basin discretization, (3) HRU definition, (4) parameter sensitivity analysis, (5) calibration and uncertainty analysis. The steps for the delineation of the watershed include DEM setup, stream definition, outlet and inlet definition, watershed outlets selection and definition and calculation of sub-basin parameters. Artificial stations were located during the setup of the SWAT model. This was aimed at quantifying the water fluxes into the lake, which could be used analyzing the water balance of the lake.

Twenty-six hydrological parameters were tested for sensitivity for the simulation of the stream flow in the study area. The data for period 1981–1992 were used for calibration and from 1993 to 2004 were used for validation of the model in the four tributaries of Lake Tana basin. Periods 1978–1980 and 1990–1992 were used as "warm-up" periods for calibration and validation purposes, respectively. The warm-up period allows the model to get the hydrologic cycle fully operational.

The calibration and uncertainty analysis were done using three different algorithms, i.e., Sequential Uncertainty Fitting (SUFI-2) (Abbaspour et al., 2004, 2007), Parameter Solution (ParaSol) (Van Griensven and Mixer, 2006) and Generalized Likelihood Uncertainty Estimation (GLUE) (Beven and Binley, 1992). The details of the methods and application can be found in Setegn et al. (2009a).

12.3 Results and Discussion

12.3.1 Future Climate Change Projection

In our analysis, we divided the data into a wet-season (June to September) and a dry-season (October to May) so that the results are easier to interpret from the perspective of possible impacts. Projected changes in seasonal mean temperature at the location of Adet station for a range of GCMs are shown in Fig. 12.4. Changes in mean seasonal accumulated precipitation are shown in Fig. 12.5. As represented by the GCMs, the Adet station can be taken to be representative of all stations in the study region, because the study area is relatively small compared to GCM resolution. Temperature changes are given in °C, and precipitation changes as a percentage change on the base-period mean (e.g. a change of 100% would imply a doubling of precipitation). This way of expressing changes has become a de facto convention. The error bars are derived from the 1-standard-deviation error-in-the-mean of seasonal average temperatures or seasonal cumulative precipitation. The error bars can be taken to represent the inter-annual variability in the models. In Fig. 12.4, the bars show plus/minus the quadrature-sum of the errors in the base-period and scenario means. The error-bars in Fig. 12.5 are derived similarly, but have been converted to percentage changes in the base-period mean. The results from Figs. 12.4 and 12.5 are summarized in Tables 12.2 and 12.3. Figure 12.4 shows that the projected temperature at Adet station for the periods 2046–2065 and

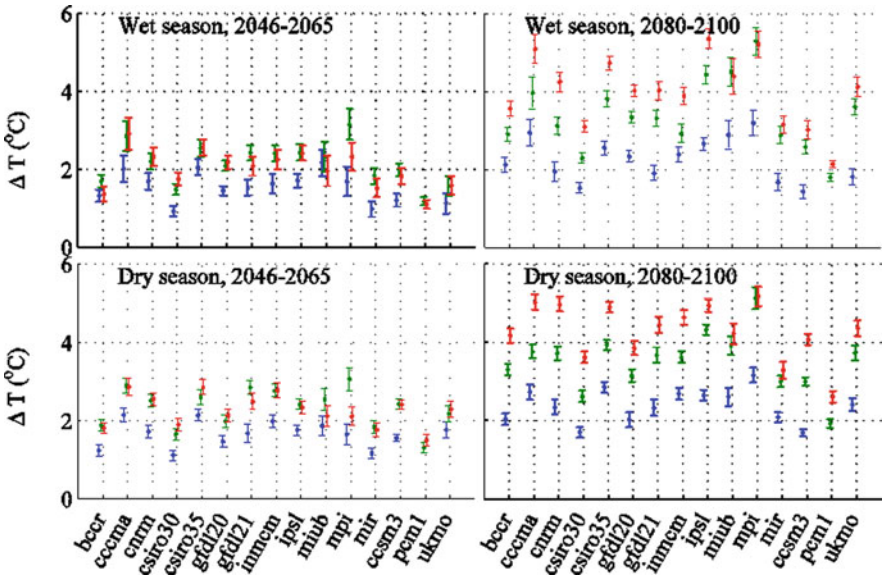

Fig. 12.4 Projected changes in mean temperature at the location of Adet station for a range of GCMs from the CMIP3 dataset. *Top row* are changes in wet-season temperature, *bottom row* are changes in dry seasons temperature. *Left column* are changes to 2046–2065, *right column* are changes to 2080–2100. Colors denote the SRES scenario used: *blue* are B1, *green* are A1b, *red* are A2. *Error bars* are 1 standard-deviation

2080–2100 for the wet and dry seasons. Figure 12.4 shows that the GCM runs project a wide range of temperature changes for the region. Even so, all the projected changes are for regional warming, and the changes are nearly all statistically-significant. In addition, the ranking of the changes for the three scenarios is consistent with what we expect. That is, for 2080–2100, the smallest changes are for the lowest-emission SRES B1 scenario, and the largest changes are for the highest-emission SRES A2 scenario.

In contrast, Fig. 12.5 suggests that the GCM's do not give us a confident picture of rainfall change in the region. Firstly, approximately half of the models suggest increases in rainfall, and half suggest decreases, so there is no consensus between GCMs. Further, in most cases the projected rainfall changes are less than 3 standard deviations; even though some of the changes are large in absolute terms (greater than 50%), we note that the larger changes are projected in the GCMs with the largest inter-annual variations. Further, for many GCMs, the changes in Fig. 12.5 are not ranked according to the emission scenarios. In fact, for several of the models the changes are similar for all three scenarios; that is, they appear to be independent of the emission scenario. This suggests that for these models the differences between the 1980–2000 base period and the future periods is partly attributable to natural variation with the base-period, because common base-period data were used for all three SRES scenarios.

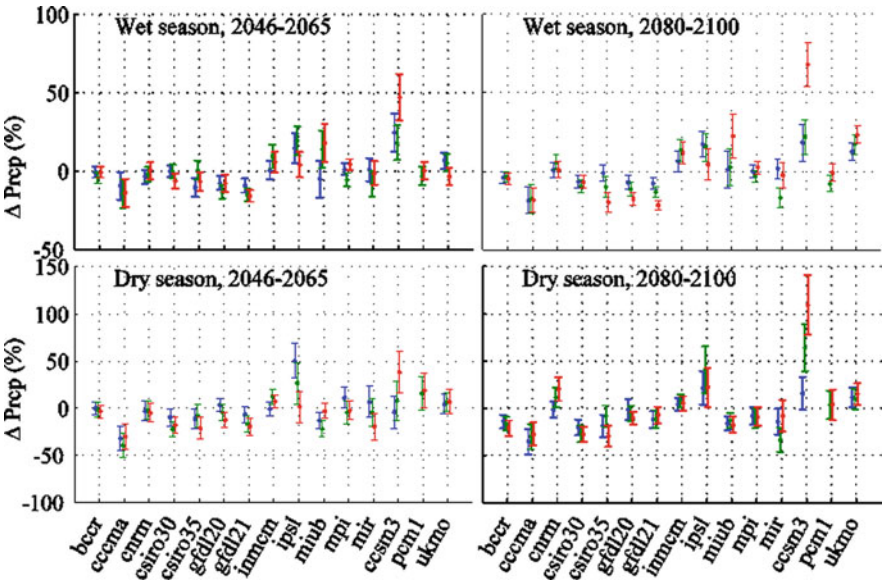

Fig. 12.5 Projected changes in mean precipitation at the location of Adet station. *Top row* are changes in wet-season precipitation, *bottom row* are changes in dry seasons precipitation. *Left column* are changes to 2046–2065, *right column* are changes to 2080–2100. Colors denote the SRES scenario used: *blue* are B1, *green* are A1b, *red* are A2. Changes are expressed as percentages of the base-period (1980–2000) precipitation. *Error bars* are 1 standard-deviation

Table 12.2 The ranges of projected changes (given as 25th–75th percentiles) for the study region for the 2080–2100 period from the 15 GCMs

	Rainfall changes		Temperature changes	
Scenarios	Wet season	Dry season	Wet season	Dry season
SRES B1	–7%–2%	–16%–11%	1.7°C–2.7°C	2.0°C–2.7°C
SRES A1b	–12%–13%	–16%–10%	2.9°C–4.0°C	3.0°C–3.9°C
SRES A2	–18%–12%	–21%–15%	3.3°C–4.7°C	3.9°C–4.9°C

Table 12.3 The ranges of projected changes (given as 25th–75th percentiles) for the study region for the 2046–2065 period from the 15 GCMs

	Rainfall changes		Temperature changes	
Scenarios	Wet season	Dry season	Wet season	Dry season
SRESB1	–8%–1%	–10%–11%	1.1°C–1.7°C	1.4°C–1.9°C
SRES A1b	–8%–9%	–17%–11%	1.7°C–2.4°C	1.9°C–2.6°C
SRES A2	–7%–4%	–20%–7%	1.6°C–2.3°C	1.9°C–2.6°C

Thus, we conclude from Fig. 12.5 that the GCMs do not project significant changes in rainfall in the region. This is not to say they do not project any changes at all. In our analysis, we compared 20-year seasonal totals, and it is quite possible that a more sophisticated statistical method that could use longer time-periods (for example regressing rainfall against global warming) would yield statistically-significant results. However, from the point-of-view of water users, our finding that the GCMs do not show consistent and statistically significant differences between the rainfall totals for the 1980–2000 period and the 2080–2100 period could be translated as "no consensus on changes in precipitation".

12.3.2 Hydrological Model Setup and Evaluation

The parameter sensitivity analysis was done using the ArcSWAT interface for the whole catchment area. Sensitivity analyses for twenty-six hydrological parameters were conducted within the study area. The most sensitive parameters considered for calibration were soil evaporation compensation factor, initial SCS Curve Number II value, base flow alpha factor, threshold depth of water in the shallow aquifer for "revap" to occur, available water capacity, groundwater "revap" coefficient, channel effective hydraulic conductivity, and threshold depth of water in the shallow aquifer for return flow to occur. The details of the sensitive flow parameters and their fitted values are documented in Setegn et al. (2009a). SUFI-2, GLUE and ParaSol methods were used for calibration of the SWAT model in Gilgel Abay, Gumera, Ribb and Megech inflow rivers. The comparison between the observed and simulated stream flows indicated that there is a good agreement between the observed and simulated discharge which was verified by high values of coefficient of determination (R^2) and Nash Sutcliffe efficiency (NSE). Model predictive performances for calibration and validation periods of all inflow rivers discharge for all calibration and uncertainty analysis methods are summarized in Setegn et al. (2009a). Figure 12.6 shows the time-series comparison between measured

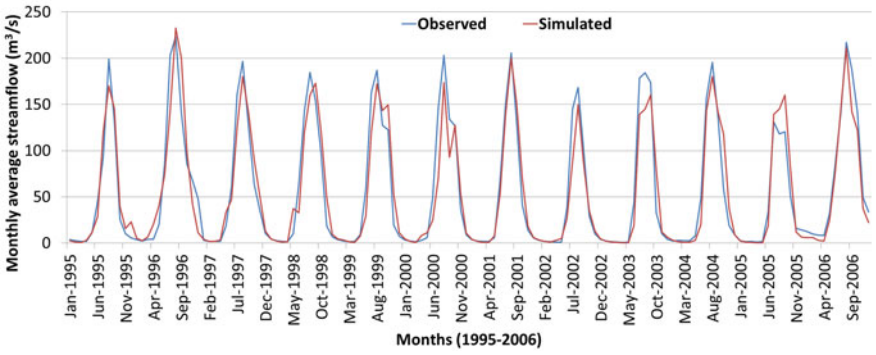

Fig. 12.6 Time series of measured and simulated monthly flow at Gilgel Abay River station for the validation period (1995–2006)

and simulated monthly flow at Gilgel Abay River gauge station during validation periods. The detailes of the calibration and validation results can be found in Setegn et al. (2009a). Setegn et al. (2009a) indicated that the water balance of the upland watershed is well represented. The results indicated that 65% of the annual precipitation is lost by evapotranspiration in the basin during the calibration period as compared to 56% during validation period. Surface runoff contributes 31% and 25% of the water yield during calibration and validation periods, respectively. Ground water contributes 45% and 54% of the water yield during calibration and validation periods, respectively.

12.3.3 Impact of Climate Change on Stream Flow

River discharge is an important hydrological component that is greatly influenced by climate (rainfall and temperature) and land use. Figure 12.7 shows the projected effect of climate change on annual stream flow, as output from the SWAT model. Using downscaled data from the CCMA, MPI and GFDL models, the streamflow showed a reduction under all SRES scenarios for both time periods (2046–2065 and 2080–2100). But with the NCAR models there was an increase in streamflow for A2 and B1 scenarios during the two time periods.

The results from the hydrological modeling for the wet-season (June-September) streamflow in the Gilgel Abay River are shown in Fig. 12.8. Wet season streamflow is significantly reduced in the downscaled cccma_cgcm3_1 model for all scenarios for both time periods. For the downscaled gfdl_cm2_1 model there are reductions of around 20% for the 2046–2065 period, and around 50% for the 2080–2100 period, with little variation between scenarios. Results from the downscaled mpi_echams5 model show little change. The downscaled ncar_ccsm3_0 model results show little

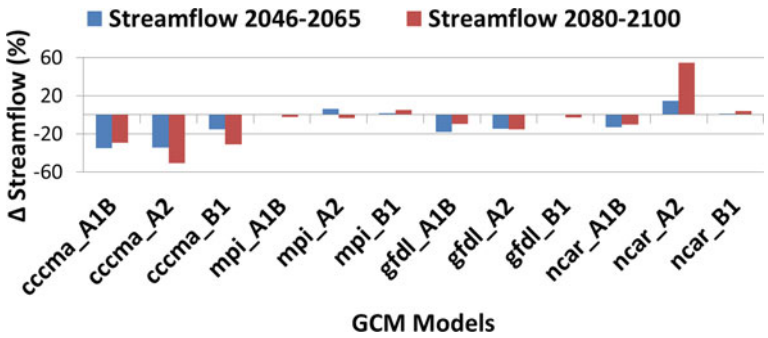

Fig. 12.7 Change in annual streamflow due to changes in precipitation and temperature for CCCMA, GFDL, MPI and NCAR models under A1B, A2 and B1 scenarios for the periods 2045–2065 and 2080–2100 expressed as a percentage of streamflow in the base period 1980–2000

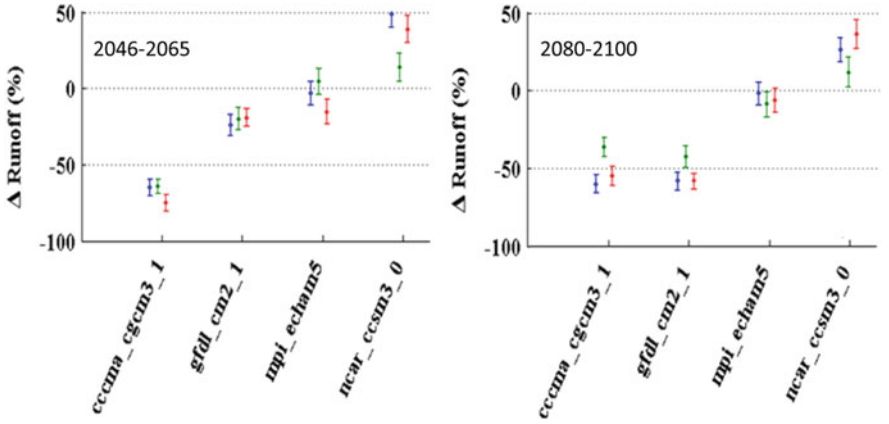

Fig. 12.8 Projected changes in wet-season runoff in the GilgelAbay River compared to the base-period 1980–2000, calculated with the SWAT model. *Left* (**a**) changes to 2046–2065, *right* (**b**) changes to 2080–2100. Colors denote the SRES scenario used: *blue* are B1, *green* are A1B, *red* are A2. Changes are expressed as percentages of the base-period (1980–2000) wet-season runoff

change, except for a streamflow increase of around 60% for the SRES A2 scenario during 2080–2100. However, of the models show similar trends across different scenarios in the 2046–2065 and 2080–2100 periods.

Although the number of GCM outputs examined in the hydrological modeling study is smaller than in the seasonal rainfall and temperature studies shown in Figs. 12.4 and 12.5 (due to both data and time constraints), we can still extract some important points. Firstly, the directions of the streamflow changes follow the changes in rainfall (i.e. decreases for the cccma_cgcm3_1 and gfdl_cm2_1 models, increases for the ncar_ccsm3_0 model for SRES A2 scenario, and no changes for the mpi_echam5 model). This is expected given the fact that local evapotranspiration does not dominate the water-cycle in the wet-season. But we also see that the streamflow changes are both larger in magnitude and more significant than the rainfall changes. We interpret these aspects of the modeling results to imply that runoff changes in the region could be significant, even though the GCMs do not agree on the direction of the change. The exceptions are the results from the ncar_ccsm3_0 model for the SRES A1B and B1 scenarios, where increases in wet-season precipitation are accompanied by streamflow declines. This is presumably not caused by unreasonable increases in modeled evaporation, because the projected temperature changes in ncar_ccsm3_0 are lower than average (see Figure 12.4). We note, however, that the ncar_ccma3_0-based simulations were downscaled using changes in the GCM daily mean temperature output (for the other models, changes in GCM daily maximum and minimum temperature were used), which may account for these anomalous results. Alternatively, the changes in precipitation and/or temperature as a function of CFD might be substantially different for the ncar_ccma3_0 outputs.

12.3.4 Impact of Climate Change on Agricultural Water Resources

In this section, we discuss changes in actual evapotranspiration (AET), soil moisture (SW) and ground water (GW) that are of the most important components of the hydrological cycle. Our intention is to understand how the changes in climate variables can affect the different hydrological components of the basin that control the final streamflow.

The possible impact of climate change on the annual changes in actual ET, soil moisture and ground water for the period of 2046–2065 and 2080–2100 periods are shown in Fig. 12.9. The results indicated that AET increases considerably in many models, but especially for GFDL model. This is attributed to the increase in air temperature. It was observed that soil moisture showed little change (between 0 and 2% decrease) for many of the models. Ground water flow is reduced for the downscaled GFDL and MPI models, but the downscaled NCAR model has shown an increase in the groundwater flow.

The increase in ET is probably due to increased air temperatures. The study used the Hargreaves algorithm (Hargreaves et al. 1985) to calculate evapotranspiration from minimum and maximum temperatures. This is consistent with previous

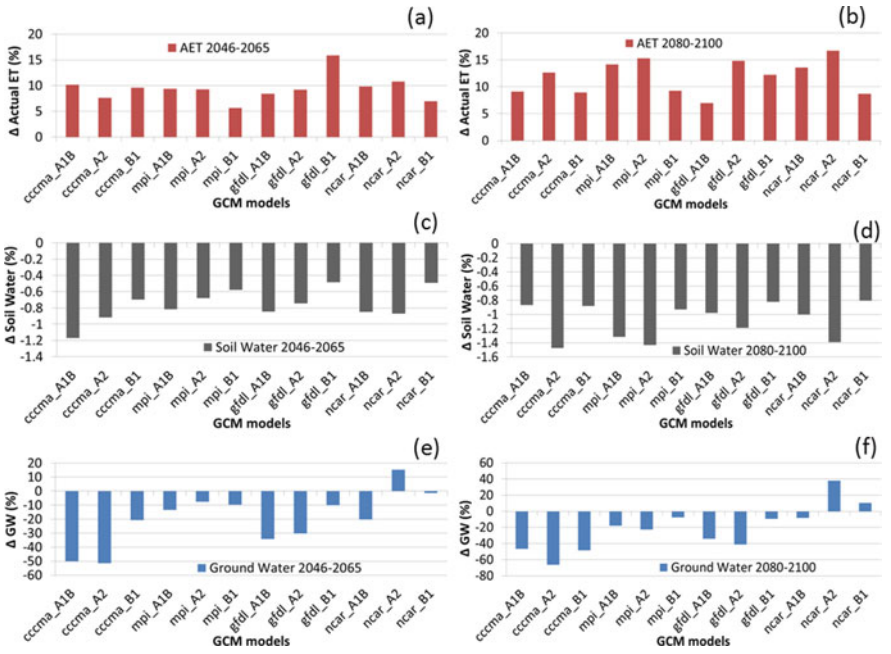

Fig. 12.9 Annual changes in actual evapotranspiration (AET), soil moisture and ground water due to changes in climate for the 2046–2065 and 2080–2100 periods: (**a**) changes in AET for 2046–2065 period, (**b**) changes in AET for 2080–2100 period, (**c**) changes in soil water content for 2046–2065 period, (**d**) changes in soil water content for 2080–2100 period, (**e**) changes in groundwater for 2046–2065 period, (**f**) changes in groundwater for 2080–2100 period

studies, which have shown that a significant variation in AET is expected to follow changes in air temperature (Abbaspour et al., 2009). The changes in modeled ground water flow clearly influenced the changes in streamflow. This is consistent with the Setegn et al. (2009a), who indicated that 60% of the stream flows from the inflow rivers of Lake Tana are baseflow, and that future reduction in ground water might contribute to reduced streamflow in the basin. Moreover, previous studies have indicated that more than 60% of the hydrological loss in the present system is through evapotranspiration. This suggests that increased evapotranspiration in the future may be a significant factor leading in the direction of decreased streamflow, which may or may not be compensated for by changes in rainfall.

In this study, we have used the same land cover data as the present time. Such a study should not be considered as a realistic actual scenario, because the latter would require including the impact of future land use change. We are conducting further investigations regarding the combined effect of climate and land use change. We note also that in the present study there is no consideration of changes in soil parameters, which could influence the soil properties of the watershed. This may explain the low response of soil moisture to the changes to climate in this study.

Considering the combined effects of land use change and climate change will also raise the question of the effect of climate change on land use changes, and vice versa. Unless we quantify the proportion of the land use changes due to human and those caused by the changing climate (rainfall and air temperature) variability, understanding the combined feedback to the water resources variability will be misleading.

There is much uncertainty in our modeling results. This is a combination of uncertainties in the GCM outputs, as a result of the downscaling, hydrological parameter uncertainty and neglect of land-use changes or potential changes in soil properties. Any or all of these factors may cause the results to deviate from reality. But even so, we are dedicated to perusing a thorough investigation of the combined effect of climate and land use/land cover on the hydrological processes and water recourses in the study area, and we believe this study is an important first-step in this direction.

12.3.5 Implications of Climate Change Impact

Ethiopia is known to be one of the countries most affected by drought. Given a large part of the country is arid or semi-arid and highly prone to drought and desertification, a further decrease in precipitation could increase the frequency and intensity of droughts in the country. Also, Ethiopia has a fragile highland ecosystem that is currently under stress due to increasing population pressure.

Our analysis suggests that the northern highlands of the country could experience reduced rainfalls, and hence become susceptible to even more severe drought conditions.

A dramatic reduction in precipitation or increase of actual evapotranspiration would cause soil moisture stress. The resulting negative agricultural water balance would reduction both rain-fed and irrigated agriculture productivity. A reduction in rainfall coupled with land degradation and other factors would also significantly reduce effective rainfall; that is, rainfall which could be available for crop consumption. The combined effect has the potential to cause a great agricultural drought, unless there is ample water available for irrigation. However, a reduction in rainfall may cause reduce ground water recharge, which would significantly reduce its contribution to stream flow. Lake Tana is highly sensitive to variations in rainfall, as well as in river inflows and evaporation. Setegn et al. (2009a) showed that inflow river discharge to Lake Tana contributes over 90% of the lake inflow. It is thus very likely that changes in river inflow would also change the volume of the lake and the water balance, which could ultimately adversely impact the lake ecosystem.

12.4 Conclusion

The possibility of a reduction in water resources is a major threat in the northern highlands of Ethiopia, due to alterations in hydrologic cycles and changes in water availability. In this study, we investigated the sensitivity of water resources to changing climate in the Lake Tana Basin, Ethiopia. We compared projected changes in precipitation and temperature across 15 GCM models for two future periods to get an indication of the consistency of the projected changes in the region. We found that the models projected temperature increases of around 2–5°C for 2080–2100, depending on the model and emission scenario. However, the models projected a wide range of rainfall changes, both increases and decreases, but the low statistical-significance of the changes combined with apparent systematic effects does not allow us to draw any definite conclusions about rainfall changes in the region. Moreover, the study investigated how changes in temperature and precipitation might translate into changes in stream flows and other hydrological components using downscaled outputs from four climate models. Although the GCM sample examined for this component of the study is small, we note important aspects of the results. Firstly, the direction of streamflow changes followed the direction of changes in rainfall. This is expected, given that local evapotranspiration does not dominate the water-cycle in the wet-season. But we also saw that the changes were both larger-magnitude and more significant than the rainfall changes. The responses of evapotranspiration, soil moisture and ground water were also examined, and it was found that changes in ground water flow may be a significant component of the changes in streamflow.

We interpret the different aspects of the hydrological response and it indicates that changes in runoff and other hydrological variables in the region could be significant, even though the GCMs do not agree on the direction of the rainfall change. This implies that climate change may well impact the surface and ground water resources of the Lake Tana Basin, and the lake may experience a change in water balance due to a change in river inflow in the forthcoming decades.

Acknowledgments We acknowledge the modeling groups, the Program for Climate Model Diagnosis and Intercomparison (PCMDI) and the WCRP's Working Group on Coupled Modelling (WGCM) for their roles in making available the WCRP CMIP3 multi-model dataset. We also would like to thank the Ministry of Water Resources of Ethiopia and the Ethiopian Meteorological Agency for the data provided and used in this study.

References

Abbaspour KC, Johnson CA, van Genuchten MTh (2004) Estimating uncertain flow and transport parameters using a sequential uncertainty fitting procedure. Vadose Zone J 3(4):1340–1352

Abbaspour KC, Yang J, Maximov I, Siber R, Bogner K, Mieleitner J, Zobrist J, Srinivasan R (2007) Modelling hydrology and water quality in the pre-alpine/alpine Thur watershed using SWAT. J Hydrol 333:413–430

Abbaspour KC, Faramarzi M, Ghasemi SS, Yang H (2009) Assessing the impact of climate change on water resources in Iran. Water Resour Res 45:W10434. doi:10.1029/2008WR007615

Abdo KS, Fiseha BM, Rientjes THM, Gieske ASM, Haile AT (2009) Assessment of climate change impacts on the hydrology of Gilgel Abay catchment in Lake Tana basin. Ethiopia 23:3661–3669

Arnold JG, Srinivasan R, Muttiah RR, Williams JR (1998) Large area hydrologic modeling and assessment: part I: model development. J Am Water Resour Assoc 34(1):73–89

Benestad RE, Chen D, Hanssen-Bauer I (2008) Empirical-statistical downscaling. World Scientific Publishing, Singapore, 300pp

Beyene T, Lettenmaier DP, Kabat P (2010) Hydrologic impacts of climate change on the Nile River Basin: implications of the 2007 IPCC scenarios. Clim Change 100:433–461

Beven K, Binley A (1992) The future of distributed models: model calibration and uncertainty prediction. Hydrol Process 6:279–298

Brown AE, Zhang L, McMahon TA, Western AW, Vertessy RA (2005) A review of paired catchment studies for determining changes in water yield resulting from alterations in vegetation. J Hydrol 310:28–61

Chang H (2003) Basin hydrologic response to changes in climate and land use: the Conestoga River Basin, Pennsylvania. Phys Geogr 24:222–247

Chorowiz J, Collet B, Bonavia F, Mohr P, Parrot J-F, Korme T (1998) The Tana basin, Ethiopia. Intra-plateau uplift, rifting and subsidence. Tectonophysics 295:351–367

Conway D (1997) A water balance model of the Upper Blue Nile in Ethiopia. Hydrol Sci J 42(2):265–286

Conway D (2000) The climate and hydrology of the Upper Blue Nile, Ethiopia. Geogr J 166:49–62

FAO (1995) Digital soil map of the world and derived soil properties (CDROM). Food and Agriculture Organization of the United Nations, Rome

FAO (1998) The soil and terrain database for northeastern Africa (CDROM). FAO, Rome, 1998.

FAO (2002) Major Soils of the World. Land and Water Digital Media Series (CD-ROM). Food and Agricultural Organization of the United Nations, Rome

Fohrer N, Haverkamp S, Eckhardt K, Frede HG (2001) Hydrologic response to land use changes on the catchment scale. Phys Chem Earth B 26:577–582

Gamachu D (1977) Aspects of climate and water budget in Ethiopia. Addis Ababa University Press, Addis Ababa

Gassman PW, Reyes MR, Green CH, Arnold JG (2007) The soil and water assessment tool: historical development, applications, and future research directions. Trans ASABE 50(4): 1211–1250

Gleick PH, Chalecki EL (1999) The impacts of climatic changes for water resources of the Colorado and Sacramento-San Joaquin River basins. J Am Water Resour Assoc 35: 1429–1441

Green WH, Ampt GA (1911) Studies on soil physics, 1. The flow of air and water through soils. J Agric Sci 4:11–24

Groisman PY, Knight RW, Karl TR (2001) Heavy precipitation and high streamflow in the contiguous United States: trends in the twentieth century. Bull Am Meteorol Soc 82: 219–246

Grotch SL, MacCracken MC (1991) The use of general circulation models to predict regional climatic change. J Clim 4:286–303

Hargreaves GL, Hargreaves GH, Riley JP (1985) Agricultural benefits for Senegal River basin. J Irrigat Drain Eng 111(2), 113–124.

Harrold TI, Jones RN (2003) Generation of rainfall scenarios using daily patterns of change from GCMs. IAHS-AISH Publ 280:165–172

Hay LE, Clark MP (2003) Use of statistically and dynamically downscaled atmospheric model output for hydrologic simulations in three mountainous basins in the western United States. J Hydrol 282:56–75

Huang MB, Zhang L (2004) Hydrological responses to conservation practices in a catchment of the Loess Plateau, China. Hydrol Proc 18:1885–1898

IPCC (Intergovernmental Panel on Climate Change) (1999) In: Penner JE, Lister DH, Griggs DJ, Dokken DJ, McFarland M (Eds.) Prepared in collaboration with the Scientific Assessment Panel to the Montreal Protocol on Substances that Deplete the Ozone Layer. Cambridge University Press, Cambridge, UK. p 373

IPCC (Intergovernmental Panel on Climate Change) (2007) In: Parry ML et al (eds) Climate change 2007: impacts, adaptation, and vulnerability—contribution of working group II to the third assessment report of the Intergovernmental Panel on Climate Change. Cambridge University Press, Cambridge, UK

International Arctic Science Committee (Content Partner); Sidney Draggan (Topic Editor) (2010) Statistical downscaling approach and downscaling of AOGCM climate change projections. In: Cleveland CJ (ed) Encyclopedia of Earth. Environmental Information Coalition, National Council for Science and the Environment, Washington, DC [First published in the Encyclopedia of Earth 8 Sept 2009; Last revised 8 Feb 2010; Retrieved 4 Sept 2010]

Kim U, Kaluarachchi JJ, Smakhtin VU (2008) Generation of monthly precipitation under climate change for the Upper Blue Nile River Basin, Ethiopia. J Am Water Resour Assoc 44(5): 1231–1274. doi:10.1111/j.1752-1688.2008.00220.x

Kim U, Kaluarachchi JJ (2009) Climate change impacts on water resources in the Upper Blue Nile River Basin, Ethiopia. J Am Water Resour Assoc (JAWRA) 45(6):1361–1378. doi:10.1111j.1752-1688.2009.00369.x

Laurance WF (1998) A crisis in the making: responses of Amazonian forests to land use and climate change. Tree 13 (10):411–415

Melesse AM, Loukas AG, Senay G, Yitayew M (2009) Climate change, land-cover dynamics and ecohydrology of the Nile River Basin. Hydrol Proc 23(26):3651–3652

Mohr PA (1962) The Geology of Ethiopia. University-College Press, Addis Ababa, 268p

Neff R, Chang H, Knight CG, Najjar RG, Yarnal B, Walker HA (2000) Impact of climate variation and change on Mid-Atlantic region hydrology and water resources. Clim Res 14: 207–218

Neitsch SL, Arnold JG, Kiniry JR, Williams JR (2005) Soil and water assessment tool, theoretical documentation: version. USDA Agricultural Research Service and Texas A&M Blackland Research Center, Temple, TX

Novotny EV, Stefan HG (2007) Stream flow in Minnesota: indicator of climate change. J Hydrol 334:319–333

Richey JE, Nobre C, Deser C (1999) Amazon River discharge and climate variability: 1903–1985, Science 246:101–103

Setegn SG, Srinivasan R, Melesse AM, Dargahi B (2009a) SWAT model application and prediction uncertainty analysis in the Lake Tana Basin, Ethiopia. Hydrol Proc 23(26):3738–3750

Setegn SG, Srinivasan R, Dargahi B, Melesse AM (2009b) Spatial delineation of soil erosion venerability in the Lake Tana Basin, Ethiopia. Hydrol Proc 24(3):357–367

Setegn SG, Dargahi B, Srinivasan R, Melesse AM (2010) Modeling of sediment yield from Anjeni-gauged watershed, Ethiopia using SWAT model. J Am Water Resour Assoc (JAWRA) 46(3):514–526. doi:10.1111j.1752-1688.2010.00431.x

Schulze RE (2000) Hydrological responses to land use and climate change: a southern African perspective. Ambio 29 (1):12–22

Tarekegn D, Tadege A (2006) Assessing the impact of climate change on the water resources of the Lake Tana sub-basin using the WATBAL model. CEEPA discussion paper no. 30, Centre for Environmental Economics and Policy in Africa, University of Pretoria

Tu J (2009) Combined impact of climate and land use changes on stream flow and water quality in eastern Massachusetts, USA. J Hydrol 379:268–283

UNESCO (United Nations Educational, Scientific and Cultural Organization) (2004) National Water Development Report for Ethiopia, UN-WATER/WWAP/2006/7. World Water Assessment Program, Report, MOWR, Addis Ababa, Ethiopia

USDA Soil Conservation Service (1972) National engineering handbook: section 4. Hydrology, Chapters 4–10 USDA-SCS, Washington, DC

Van Griensven A, Meixner T (2006) Methods to quantify and identify the sources of uncertainty for river basin water quality models. Water Sci Technol 53(1):51–59

Van Roosmalen L, Sonnenborg TO, Jensen KH (2009) Impact of climate and land use change on the hydrology of a large-scale agricultural catchment. Water Resour Res 45:W00A15. doi:10.1029/2007WR006760

Van Wambeke A (2003) Properties and management of soils of the tropics, FAO Land and water digital media series no. 24. FAO, Rome

Wilby RL, Wigley TML, Conway D, Jones PD, Hewitson BC, Main J, Wilks DS (1998) Statistical downscaling of general circulation model output: a comparison of methods. Water Resour Res 34(11):2995–3008

Wilby RL, Hay LE, Gutowski WJ, Arritt RW, Takle ES, Pan Z, Leavesley GH, Clark MP (2000) Hydrological responses to dynamically and statistically downscaled climate model output. Geophys Res Lett 27(8):1199–1202

Williams JR (1995) The EPIC model. In: Singh VP (ed) Computer models of watershed hydrology. Water Resources Publications, Highlands Ranch, CO, Chapter 25, pp 909–1000

Wood RB, Talling JF (1988) Chemical and algal relationships in a salinity series of Ethiopian inland waters. Hydrobiologia 158:29–67

Wood AW, Leung LR, Sridhar V, Lettenmaier DP (2004) Hydrologic implications of dynamical and statistical approaches to downscaling climate model outputs. Clim Change 62:189–216

Wudneh T (1998) Biology and management of fish stocks in Bahir Dar Gulf, Lake Tana, Ethiopia. PhD dissertation. Wageningen Agricultural University, Wageningen, 144p

Zhang L, Dawes WR, Walker GR (2001) The response of mean annual evapotranspiration to vegetation changes at catchment scale. Water Resour Res 37:701–708